Femtosecond Dynamics of Unimolecular and Unrestricted Bimolecular Reactions

Una Marvet, Qingguo Zhang,† and Marcos Dantus*

Department of Chemistry and Center for Fundamental Materials Research, Michigan State University, East Lansing, Michigan 48824-1322

Received: October 10, 1997; In Final Form: December 10, 1997

The results of two time-resolved experiments using femtosecond laser pulses are presented. In the first, molecular photoinduced detachment of I_2 from methylene iodide is studied. The progress of the reaction is monitored by selective detection of fluorescence from the iodine product; molecular dynamics are probed by depletion of the fluorescent state. Pump−probe spectroscopy of the halogen moiety following high-energy (12 eV) excitation reveals that the reaction proceeds by a concerted asynchronous mechanism. The second experiment is a real-time study of an unrestricted bimolecular reaction. In this process, gas phase mercury atoms are photoassociated to an electronically excited state using a femtosecond pulse; the real-time dynamics of the resulting excimers are probed by fluorescence depletion using a second pulse. Analysis of the rotational anisotropy in the nascent dimers reveals the degree of rotational excitation in the excited state and indicates the impact parameter selectivity of the photoassociation process.

I. Introduction

Femtosecond time-resolved studies are used increasingly to reveal the dynamics of primary reaction steps such as bond breaking, electron transfer, proton transfer, and isomerization in gaseous and condensed phases.[1−4] Two types of experiments are presented in this paper. The first experiment is a study of concerted molecular detachment involving the formation and breakage of multiple chemical bonds, and the second explores the time-resolved dynamics of unrestricted bimolecular reactions.

High-energy (>9 eV) excitation of CH_2I_2 has been found to open a minor dissociation channel which leads to the formation of molecular iodine in its electronically excited ion-pair states.[5−9] Unlike the low-energy dissociation channels, which produce atomic iodine, the high-energy molecular detachment process requires breakage of two C−I bonds along with formation of an I−I bond. Understanding of this process is important in terms of unraveling similar types of reactions, e.g. the production of H_2 from NH_3, H_2O, H_2CO, and CH_4;[10] Cl_2 from $COCl_2$;[11] IBr from CH_2IBr;[12] and O_2 from OClO.[13,14] Thus, part of this study will be devoted to detailed analysis of the dynamics of the molecular detachment channel of CH_2I_2 photodissociation.

In a recent publication, Marvet and Dantus reported on the high-energy (12 eV) dissociation dynamics of CH_2I_2.[15,16] Most of the iodine formed was found to be in the fluorescent D′-($^3\Pi_{2g}$) state. Depletion probing of the D′ → A′ emission revealed a fast dissociation process (τ_{diss} < 50 fs)[17] to produce vibrationally excited I_2 molecules. The observation of vibrational coherence in the nascent I_2 provided direct evidence on the concertedness for this molecular detachment process. In this paper, we present the results of time-resolved experiments designed to investigate a second channel, which produces I_2 in the f($^3\Pi_{0g}^+$) state. We find that this pathway results in a high degree of rotational excitation in the products, implying that the dissociation mechanism that produces I_2 in the f state is concerted but not synchronous.

The experiment described above is a study of a unimolecular photodissociation reaction. This type of process involves absorption of a photon by a molecule, resulting in the formation of fragments. By contrast with this, photoassociation occurs when the absorption of a photon by a collision pair induces bond formation.[18−22] This process can be described as truly bimolecular when the reactants are free and unbound prior to initiation of the reaction. Photoassociation spectroscopy has been used for a number of purposes, for example to study the electronic excited states of species having repulsive ground states.[23−27] A number of studies also exist on long-range interactions between ultracold atoms in order to elucidate details about the ground-state potential of alkali metal dimers near the dissociation limit.[28−32] However, these studies are not time-resolved.

There are a number of theoretical studies on the possibility of directly probing photoassociation dynamics in real time.[33−35] A femtosecond time-resolved study of I_2 and Xe has been performed.[36] Unlike unimolecular reactions, which are generally amenable to study by time-resolved methods, real-time observation of photoassociation reactions presents difficulties. There are several reasons for this. Since the pulse has a short time duration, the number of collision pairs which can be associated within the pulse essentially depends on the spatial distribution and relative momenta of the atoms at the moment when the pulse is switched on. In a gas phase sample this number may be prohibitively small. A more fundamental problem arises as a result of the nature of the ground state, which is composed of a thermal ensemble of continuum states. As a result of this, the possibility of preparing a well-defined wave packet on the excited state potential energy surface is not immediately obvious. Finally, definition of a "time zero" or initiation time for the bimolecular reaction is ambiguous because the atoms are undergoing random motion. These drawbacks have to some extent been circumvented by the use of precursors.[37−40] These are generally van der Waal's complexes which undergo a full

* Corresponding author. E-mail: dantus@cem.msu.edu.
† Present address: George R. Harrison Spectroscopy Laboratory, Massachusetts Institute of Technology, Cambridge, MA 02139-4307.

S1089-5639(97)03297-0 CCC: $15.00
Published on Web 01/30/1998

collision reaction upon liberation of one of the reactants from the complex, or photoactivation of an atom.[41] In this way the collision geometry and initiation time of the reaction are clearly defined.

Experiments performed in this laboratory on the formation of excited mercury dimers have demonstrated the use of pump−probe femtosecond methods to study the molecular dynamics of photoassociation reactions in real time.[42,43] In these studies, a femtosecond pulse was used to excite pairs of mercury atoms from an essentially repulsive ground state to a bound excited electronic state, thereby forming a bond between them. The molecular dynamics of the nascent excimers were probed by using a second femtosecond pulse to deplete the observed fluorescence. Rotational anisotropy was observed as a result of the polarization of the binding laser; this was taken as evidence that mercury dimers were being formed within the duration of the pulse. Subsequent theoretical studies have provided further confirmation on this interpretation.[44−47] The short time duration of the pulse determines the initiation time of the reaction, and the restrictive Franck−Condon factor of the photoassociation transition produces a sufficiently narrow wave packet on the excited-state potential energy surface for vibrational and rotational dynamics to be resolved. In this paper we present results from femtosecond photoassociation studies of the mercury excimer formation process, including analysis of the rotational anisotropy. It is demonstrated that the wavelength of the binding pulse can be used to restrict the reaction to a narrow range of impact parameters, which produces a characteristic rotational population in the product molecules.

II. Experimental Section

The laser system used was a home-built colliding pulse mode-locked dye laser (CPM), pumped by an Ar^+ laser. The output from the CPM was amplified and recompressed to produce transform-limited 60 fs pulses centered at 624 nm, having an energy of 0.5 mJ per pulse and a repetition rate of 30 Hz. The pulses were then split by a Mach-Zhender interferometer arrangement with one fixed and one adjustable arm; 312 nm pulses were generated in the fixed arm by frequency doubling using a 0.1 mm KDP crystal. Pump and probe pulses, attenuated to <10 μJ per pulse, were collinearly recombined and focused (200 mm) in the sample cell. For both experiments, detection was by fluorescence collected perpendicular to the direction of propagation of the laser. The signal obtained at each time delay between the pump and probe pulses was averaged for 10 laser shots. Typical transients contained data from 200 different time delays and were averages of 100 scans.

CH_2I_2 (Aldrich, 99% purity) was introduced to a quartz cell and outgassed to 10^{-5} Torr at liquid nitrogen temperatures prior to each experiment. The purity of the samples was checked using FTIR and GC-MS. Experiments were carried out at room temperature, at a vapor pressure of 1 Torr, and in the presence of iodine scavenging agents (copper and sodium thiosulfate) to ensure that the signal originates from nascent iodine only.

The mercury sample, triply vacuum distilled and certified to contain a total of less than one part per million impurities (Bethlehem Apparatus Co.), was introduced to a thoroughly cleaned and vacuum-baked glass line by injection over an argon atmosphere. The injection port was sealed and the sample pumped to 10^{-5} Torr. A portion of the line containing the quartz cell and a U trap was then closed to the rest of the pumping station and immersed in liquid nitrogen to achieve cryopumping while the cell was sealed off. The purity of the sample was checked by LIF in the 190−850 nm region at high laser intensity. Fluorescence from the cell showed two Hg_2 bands and some atomic mercury lines (resulting from multiphoton excitation); we found no spectral evidence of contamination in the sample. The cell was wrapped in heating tape and maintained at a constant temperature throughout the experiment. Most of our results were obtained at 160 °C, which corresponds to a mercury vapor pressure of 4.2 Torr.[48]

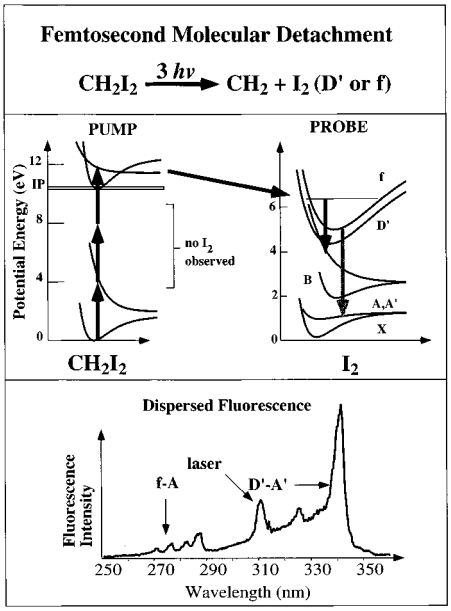

Figure 1. (top) Pump−probe scheme employed for interrogating the molecular detachment of I_2 from CH_2I_2. The three-photon pump (at 312 nm) excites the parent molecule to a dissociative state producing I_2 in the D′ and f states. The probe laser (at 624 nm) depletes the population in the D′ and f states thereby reducing the observed fluorescence. (bottom) Dispersed fluorescence spectrum resulting from the excitation of CH_2I_2 with a femtosecond laser at 312 nm. Most of the signal at wavelengths longer than 290 nm can be assigned to the D′ → A′ transition. Spectral features in the 260−290 nm region are tentatively assigned to the I_2 f → A emission although contributions from the F → X transition are also possible.

III. Results and Discussion

A. Photodissociation Dynamics of CH_2I_2. The photodissociation of CH_2I_2 from excited electronic states has been studied extensively.[5−9] Only recently have the high-energy dynamics of this molecule been investigated using femtosecond time resolution.[15,16] Since the observation of the concerted elimination of I_2 from CH_2I_2, we have conducted a series of experiments, designed to elucidate the dynamics of various photodissociation channels of CH_2I_2 and its dihaloalkane analogues.[17] In this paper we present results from two molecular detachment pathways of CH_2I_2.

Presented in Figure 1 is a dispersed fluorescence spectrum obtained by exciting a sample of neat CH_2I_2 vapor at room temperature, using femtosecond pulses with a spectrum centered around 312 nm. Nearly all the spectral features in Figure 1 can be attributed to fluorescence of the I_2 photofragments. In particular, the intense features from 290 to 350 nm are due to the I_2 D′ → A′ band system[49,50] while the weaker features below 290 nm can be assigned to the I_2 f → A and/or F → X systems.[51,52] On the basis of analysis of the vibrational dynamics of this channel, we determined that the most likely source of this fluorescence is the f → A transition;[17] the following discussion will therefore assume that this is the case. The integrated intensity of the 290 nm fluorescence is about 10 times

weaker than that of the D′ → A′ system. As pointed out by Okabe and co-workers,[8] formation of molecular I_2 from photodissociating CH_2I_2 represents only a minor photodissociation channel, with a branching ratio of approximately 1%. Thus, we estimate the overall yields of the following dissociation channels:

$$CH_2I_2 + 3h\nu(312\text{ nm}) \rightarrow CH_2 + I_2(D'\,^3\Pi_{2g}) \quad (1A)$$

$$CH_2I_2 + 3h\nu(312\text{ nm}) \rightarrow CH_2 + I_2(f\,^3\Sigma_{0_g}^+) \quad (1B)$$

to be approximately 1% and 0.1%, respectively. Since production of I_2 molecules in the D′ and f states from a thermal sample of CH_2I_2 requires minimum energies of 8.38 and 9.20 eV, respectively, at least three 312 nm photons are needed in each case to supply the necessary energy.[53,54] Preliminary power dependence results also seem to support this conclusion. The following analysis is therefore made assuming that the excitation is a three-photon process.

The pump−probe scheme depicted in Figure 1 has been employed to interrogate the photodissociation processes in (1). Here, three-photon excitation by a femtosecond laser pulse at 312 nm (pump) promotes CH_2I_2 to its highly (∼12 eV) excited electronic state(s). At such high electronic excitation, CH_2I_2 dissociates via numerous pathways, two of which produce I_2 in its D′ and f states. A second femtosecond laser pulse at 624 nm then probes this dissociation process by selectively monitoring the decrease in the fluorescence of the nascent I_2 photofragments at 340 nm (D′ → A′) or 272 nm (f → A). Sweeping the time delay between the pump and probe pulses thus yields a transient that reflects the temporal evolution of the dissociation process and that of the nascent I_2 photofragments.

Time data obtained in this way from the dissociation of CH_2I_2 are presented in Figure 2. Figure 2a shows the transients detected at 340 nm (D′ → A′ fluorescence) and Figure 2b the 272 nm (f → A fluorescence) of nascent I_2. There are two traces shown in each panel. The thicker trace was taken with the pump and the probe polarized parallel to each other. The lighter trace was taken with the probe polarization rotated 90° from the pump polarization. All transients show depletion of fluorescence signals at positive time delays, where the probe pulse arrives later than the pump pulse.

Oscillatory variations in fluorescence signal as a function of pump−probe time delay are also clearly visible in all transients at positive times. This variation can be interpreted as the signature of the *coherent* vibrational motion imparted on the nascent I_2 fragments during the dissociation process. The observed vibrational coherence in the I_2 fragment implies that the I_2 elimination process is concerted; i.e., I−I bond formation and the two C−I bond breakages happen in a single kinetic step. This, however, in no way implies that the three elementary events happen synchronously. In fact, some of the following discussion will address the timing of these events.

As shown in the inset of Figure 2a, the 340 transients display a large time zero feature, which is caused by a cooperative multiphoton process occurring when pump and probe pulses are overlapped in time. This feature conceals any dynamics occurring during the first 300 fs after time zero. The transients in Figure 2b show no time-zero feature. Examination of the data in Figure 2b reveals that depletion immediately after time zero is more efficient when the pump and probe pulses are polarized perpendicular to each other than when they are parallel. This indicates that the dipole moment of the probe transition is perpendicular to that of the pump transition at time zero. It is apparent from Figure 2b that there is a considerable degree of anisotropy in the data, most of which decays during the first 500 fs after formation of the I_2 photodissociation product. The fast decay indicates a high degree of rotational excitation in the I_2 fragment.

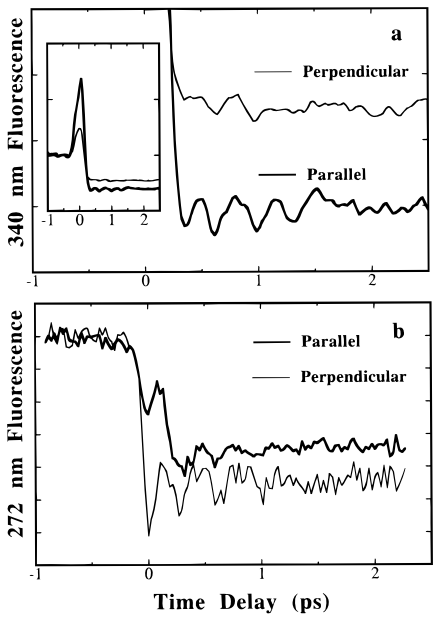

Figure 2. Femtosecond transients obtained for the dissociation of CH_2I_2 using the pump−probe scheme shown in Figure 1. (a) Nascent I_2 fluorescence is collected at 340 nm, the wavelength of maximum signal for the D′ → A′ emission. The heavy (thin) line corresponds to data collected for parallel (perpendicular) pump/probe polarization. The inset shows the overall time behavior of the tranisent including an intense feature near time zero. The expanded transient displays oscillatory features corresponding to vibrational coherence in the I_2 product. (b) Femtosecond transients obtained from CH_2I_2 when the dispersed fluorescence is collected at 272 nm, the maximum for the f → A emission. The heavy (thin) line corresponds to data collected for parallel (perpendicular) pump/probe polarization. Notice that this time the depletion in the perpendicular signal is more pronounced than the parallel (see text). The transient displays oscillatory features corresponding to vibrational coherence in the I_2 product and the differences between parallel and perpendicular transients are analyzed for rotational anisotropy.

In order to obtain more quantitative information on this fast decay of rotational anisotropy, we have extended the formulation for one-photon pump and one-photon probe by Baskin and Zewail[55] to the more general case of multiphoton pump and probe. A detailed derivation will be presented elsewhere.[17] For the case of three-photon pump and one-photon depletion probe, we have found that the rotational anisotropy $r_\perp(t)$ can be expressed as

$$r_\perp(t) = -\frac{1}{12} - \frac{1}{4}\frac{\sum_j P_j \cos(2\omega_j t)}{\sum_j P_j} \quad (2)$$

Here the subscript ⊥ signifies that at time zero the pump and probe dipoles are perpendicular to each other. P_j denotes the relative rotational population distribution, which we will assume to be Gaussian. The j-dependent frequency ω_j equals $4\pi Bj$, where B denotes the rotational constant and j the rotational quantum number of the molecules. Least-squares fitting of the rotational anisotropy shown in Figure 2b yields a rotational distribution having a central value $j_{max} = 354 \pm 38$ and a $1/e$ width $\Delta j = 509 \pm 52$.

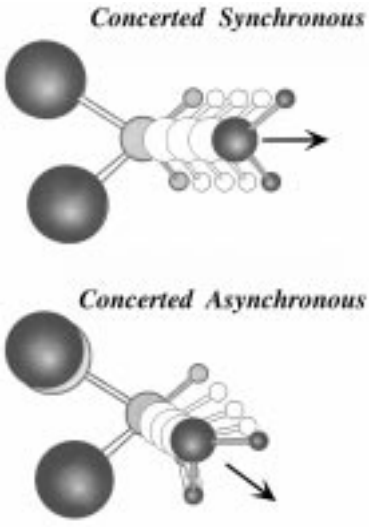

Figure 3. Schematic view of the two types of concerted mechanisms considered for the molecular detachment pathways during the first ~50 fs. The *concerted synchronous* mechanism requires that breakage of the two C−I bonds and formation of the I−I bond occur at the same time. This mechanism does not yield a high degree of rotational excitation in the fragments. The *concerted asynchronous* mechanism requires that one of the C−I bonds breaks before the other. This mechanism causes a large amount of rotational excitation in the fragments and is consistent with the observed anisotropy in the data of the CH_2I_2 (f $^3\Pi_{0g}^+$) dissociation channel.

For a room-temperature sample of CH_2I_2, the average rotational quantum number is expected to be approximately 100. This is much smaller than the measured rotational distribution of the I_2 product. Conservation of angular momentum demands that the difference, about 250$\hbar$, be taken up by the CH_2 fragment. This can be accounted for if one of the two C−I bond-breaking processes happens earlier than the other. This would exert a large torque on the fragments, causing them to exhibit counter rotation and a high degree of rotational excitation. The strong torque and available excess energy would break the second C−I bond. This corresponds to the concerted asynchronous mechanism shown in Figure 3. By contrast, if the photodissociation process proceeded by the concerted synchronous mechanism, one would not expect to observe high rotational excitation in either fragment.

Thus, we can construct the following picture of the photodissociation dynamics of CH_2I_2 to produce I_2 in the f state at an excitation energy of 12 eV. A three (312 nm) photon transition excites CH_2I_2 molecules from the thermally populated ground electronic state to a dissociative state. One of the C−I bonds breaks and a bond forms between the two iodine atoms (see the concerted asynchronous mechanism in Figure 3); this generates an enormous amount of torque on the CH_2 and I_2 moieties to tear the second C−I bond apart. This mechanism is quite in keeping with the mechanism proposed by Hoffmann and co-workers,[56] although the latter was proposed for CX_2Y_2 dissociation from the low-energy potential surfaces. Due to the time zero feature when the detection wavelength is set at 340 nm, the rotational anisotropy information at early times is masked and it is not certain whether or not the concerted asynchronous mechanism also applies to the I_2 (D′) dissociation channel of CH_2I_2.

B. Unrestricted Bimolecular Reactions. When a pulse of sufficiently short time duration excites a molecule, a coherent superposition of eigenstates or wave packet is produced. This makes it possible to study molecular dynamics using pump−probe spectroscopy, and there is now a large body of work in the literature in which ultrashort pulses are used to study the dynamics of bound → free or bound → bound transitions in this way.[1−4] In the case of a free → bound (photoassociation) transition, where the initial excitation is from a set of continuum states, well-localized wave packets can be formed on the excited state surface as long as there is a large enough difference in the slope between the upper and lower electronic states. The Franck−Condon factors of the transition dictate that photoassociation probability is greatest when the laser wavelength is resonant with the energy difference between the ground and excited state energies, which imposes a spatial and energetic restriction on the reaction. Tuning of the wavelength of the binding pulse can thus be used to select a range of reactive impact parameters. Temporal resolution is afforded by the binding pulse and is limited only by the pulse duration. Molecular dynamics following photoassociation can thus be probed using the same techniques that have been used for bound → free or bound → bound transitions.[42,43] Results are presented below on the application of this method to the formation of Hg_2*.

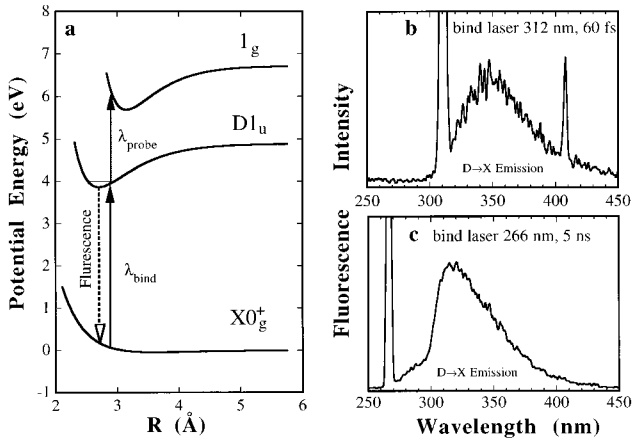

Figure 4. (a) Schematic of the potential energy surfaces relevant to the femtosecond photoassociation of Hg atoms. Only collision pairs that are in resonance with the binding laser at 312 nm and are oriented parallel to the polarization of the pulse are photoassociated to the D 1_u state. The D → X fluorescence is used to monitor the time evolution of the encounter. The population in the D state is depleted by a 624 nm probe pulse. (b) Dispersed fluorescence spectrum resulting from excitation with a 60 fs laser pulse centered at 312 nm. The peak at 407.8 nm is an atomic line resulting from two-photon excitation to the 7^1S_0 state. (c) Fluorescence spectrum resulting from the excitation of mercury vapor at 266 nm with a nanosecond laser pulse. The D → X emission is blue-shifted compared to the emission produced by 312 nm excitation because of the difference in excitation energy.

The relevant Morse potentials of Hg_2 are shown in Figure 4a. Absorption of a femtosecond laser pulse at 312 nm causes photoassociation from the essentially repulsive $X0_g^+$ state to the bound D 1_u state.[57,58] Excitation to the D 1_u state was experimentally confirmed by observation of the D → X molecular fluorescence as shown in Figure 4b. The spectrum produced by excitation at 266 nm (nanosecond pulse) is also presented in Figure 4c for comparison; this spectrum is characteristic of Hg_2 D → X fluorescence.[58−60] To observe time-dependent behavior, molecular dynamics were probed by using a 624 nm pulse to deplete the D 1_u fluorescence to the 1_g state.

The transients obtained from mercury vapor with 312 nm excitation and 624 nm probing are shown in Figure 5. At negative times, the fluorescence signal produced by photoassociation into the D 1_u state is unaffected by the depletion

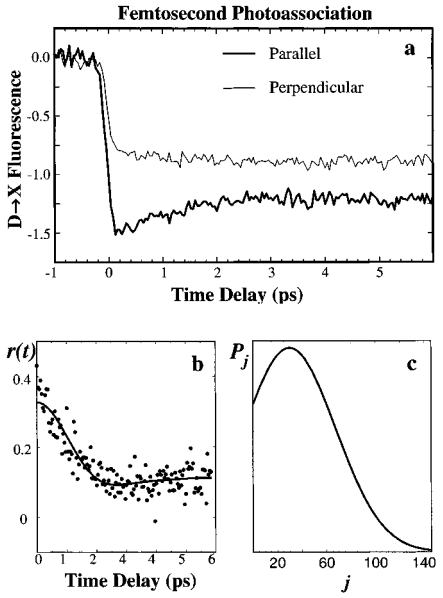

Figure 5. (a) Femtosecond transients from the photoassociation of mercury at 312 nm. The heavy (thin) line corresponds to parallel (perpendicular) polarization of the bind and probe pulses relative to each other. Note that bond formation occurs during the pulse and that the data is clearly anisotropic, indicating alignment of the photoassociated collision pairs. (b) Rotational anisotropy $r(t)$ obtained from the experimental data. The heavy line is the best fit to the experimental data (plotted as points), as described in the text. (c) Rotational population of the photoassociated product, obtained from the fit to the rotational anisotropy.

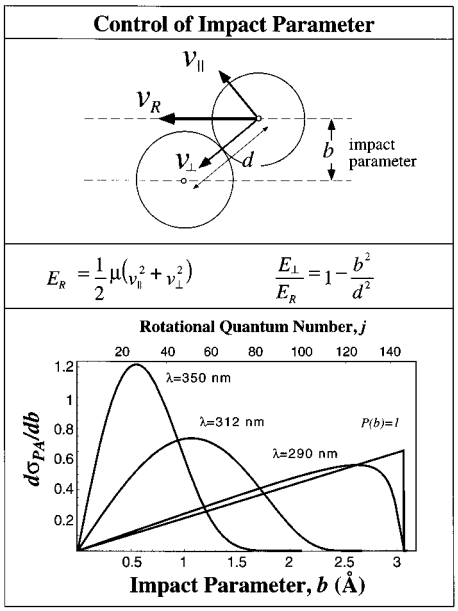

Figure 6. Schematic of a bimolecular collision process, illustrating the definition of the impact parameter b. The equations show the relation between the relative energy of collision E_R and the energy $E_\perp$ along the direction of the interatomic axis as a function of the impact parameter. The differential photoassociation cross section $d\sigma_{PA}/db$ from eq 8 is plotted as a function of binding wavelength. Note that as the wavelength is tuned to lower energies the reaction requires smaller impact parameters and the products are formed with a narrower, lower energy distribution of rotational excitation. At 290 nm the photoassociation process is not very restrictive and approaches the theoretical limit $P(b) = 1$ (see text).

(probe) pulse, which precedes it. As time zero is approached, depletion of the molecular fluorescence begins to be apparent as molecules in the D 1_u state are excited into the 1_g state by the 624 nm pulse. Transients were obtained with the polarization vectors of the pump and probe pulses aligned parallel or perpendicular to each other. The anisotropy in the data arises as a result of the preferential photoassociation of collision pairs that are aligned parallel to the polarization of the binding pulse (parallel transition). The observed anisotropy indicates rotational coherence in the nascent excimers and can only be interpreted as due to photoassociation of the free mecury atoms within the duration of the pulse.[42,45] The collisional association of excited atoms Hg* + 2Hg or Hg* + $Hg_2 \rightarrow Hg_2$* + Hg or the direct excitation of existing dimers can be ruled out as potential sources of the observed signal based on the following observations. The former requires three-body collisions, which are highly improbable and occur over a period of nanoseconds under experimental conditions. Molecular dynamics on the femtosecond time scale could not possibly be observed if this were the mechanism; since collisional association of atoms is an inherently isotropic process there would also be no rotational anisotropy in the data. The contribution to the signal from the direct excitation of van der Waals dimers is negligible because their concentration is very low (~10 ppm) under the experimental conditions. This, combined with the Franck−Condon factors for excitation of these dimers to the D 1_u state at 312 nm ($<10^{-14}$),[61] makes bound → bound transitions highly improbable.

The rotational anisotropy of the transients can be extracted using the weighted difference

$$r(t) = \frac{I_{||} - I_\perp}{I_{||} + 2I_\perp} \tag{3}$$

as shown in Figure 5b.[62] The observed dephasing of rotational anisotropy can be analyzed using a simple model which treats the rotational population P_j as a Gaussian:

$$r(t) = \sum_{J=0}^{\infty} r(j,t)P_j \tag{4}$$

where

$$P_j = \frac{2\sqrt{\ln 2}}{\Delta j\sqrt{\pi}} \exp\left\{-4 \ln 2\left(\frac{j - j_{max}}{\Delta j}\right)^2\right\} \tag{5}$$

$$r(j,t) = 0.1 + 0.3 \cos(2\omega_j t) \tag{6}$$

where $\omega_j = 4\pi Bj$ is the molecular rotational frequency.[55] Least-squares fitting to the data indicates that the rotational excitation can be modeled with a rotational distribution centered at $j_{max} \approx 30$ and a fwhm Δj of ≈90, as shown in Figure 5, b and c.

In order for photoassociation to occur, the relative collision energy of an atom pair with a given impact parameter b (as defined in Figure 6) should satisfy the condition

$$E_{rel} \geq \frac{V_1(R')}{1 - (b/R')^2} \tag{7}$$

where $V_1(R')$ is the potential energy of the ground state and R' the internuclear distance at which the laser is resonant with the transition from the ground to the upper electronic state.[46] An expression can be derived for the differential photoassociation cross section $d\sigma_{PA}/db$ using the well-known expression for the scattering cross section:

$$d\sigma_{PA}/db = 2\pi bP(b) \tag{8}$$

where $P(b)$ is the opacity function.[63] Integration over the Boltzmann population of scattering states, taking into account the energetic restriction in eq 7, results in

$$P(b) = \exp\left\{-\frac{V_1(R')}{[1-(b/R')^2]k_BT}\right\}$$

Figure 6 shows plots of $d\sigma_{PA}/db$ for three values of binding wavelength. Note that at 350 nm, only those collision pairs with very small impact parameters are photoassociated. As the binding laser is tuned to shorter wavelengths, the position of highest photoassociation probability shifts to larger impact parameters and the selectivity is lost. The opacity function in eq 9 reaches a limiting value $P(b) = 1$ at high excitation energies, when $V_1(R')$ approaches zero. This behavior is also shown in Figure 6 for comparison.

The restrictions on impact parameter imposed by eq 9 are reflected in the rotational quantum numbers of the product molecules. The conversion from impact parameter to angular momentum is obtained by using the quantum-to-classical conversion $j\hbar = \mu v b$, where v is the relative velocity of the atoms when they are photoassociated. Figure 6 was plotted using the mean relative velocity $\bar{v}$. Under experimental conditions ($\lambda_{bind} = 312$ nm, $R' = 2.82$ Å), it can be seen that the predicted parameters are $j_{max} \approx 50$ and $\Delta j \approx 65$. A number of assumptions inherent in the model may be responsible for the discrepancy between the experimental and theoretical rotational distribution; see Figure 5, b and c. The larger Δj in the experimental data may be due to the use of a single average value for the relative velocity of the atoms rather than the thermal distribution. A slight saturation of the photoassociation transition by the laser may also make the rotational distribution appear to be broader than it actually is.

Quantum mechanical simulations of this work indicate that it is also possible to observe vibrational coherence in the photoassociated molecules.[44−46] However, the modulation depth of these coherences is not large and we have to date been unable to unambiguously identify vibrations in the pump−probe data.

IV. Conclusion

Results were presented of a femtosecond pump−probe experiment on a molecular photodetachment process. Product coherence resulting from the concerted elimination of molecular iodine on photolysis of CH_2I_2 was demonstrated. Least-squares fitting of the rotational anisotropy in the transients obtained from I_2 in the f state to a Gaussian distribution of rotational level occupations revealed a distribution of rather high I_2 rotational levels, with the distribution center at around $j_{max} = 354 \pm 38$ and a $1/e$ width $\Delta j = 509 \pm 52$. This high degree of rotational excitation has been explained by invoking a concerted sequential I_2 detachment mechanism (see Figure 3). When CH_2I_2 is excited to a highly electronically excited dissociative state, one of the two C−I bonds breaks and an I−I bond forms. Then the second C−I bond ruptures, leaving rotationally excited I_2 and translationally hot CH_2 fragments. The high degree of rotational excitation in the I_2 in the f state product rules out the concerted simultaneous mechanism shown in Figure 3 as a possible mechanism for this reaction. If this were the reaction pathway, C_{2v} symmetry would be maintained throughout the dissociation and there would be little rotational excitation in either fragment.

Results were also presented of an unrestricted bimolecular (photoassociation) reaction, studied by a femtosecond pump−probe method. In this case, excitation from a set of continuum states to a bound electronically excited state produces coherent wave packets on the upper state. This allows the molecular dynamics of the reaction and nascent products to be studied in real time by fluorescence depletion probing. The energy restrictions imposed on the photoassociating molecules by the resonance condition with the binding pulse can be used to select a range of collision impact parameters, which in turn determines the rotational excitation in the product. It was determined that, under the conditions of the experiment, the rotational excitation in the mercury dimers can be fit to a Gaussian distribution having a maximum at $j_{max} \approx 30$ and a fwhm Δj of ≈90.

The experimental information obtained from unimolecular photodissociation (half collision) reaction is limited by the well-defined initial geometry. This, in terms of molecular scattering, translates into a single value of the impact parameter. Unrestricted encounters occurring in bimolecular reactions, however, sample the whole range of impact parameters and molecular orientations. Information about these encounters is not accessible from the study of unimolecular dissociation reactions, and therefore, time-resolved studies of photoassociation are of importance. As shown in this work, one is able to study the real time dynamics from limited ranges of impact parameters by the appropriate choice of photoassociation wavelength. Work is continuing in this laboratory on the real time study of unrestricted bimolecular reactions. Of particular interest is the study of atom + diatom reactions for which orientation as well as alignment should have a significant effect on the nature and energetics of the products.

Acknowledgment. This research was partially funded by a Camille and Henry Dreyfus New Faculty Award. M.D. is an Arnold and Mabel Beckman Young Investigator and a Packard Science and Engineering Fellow.

References and Notes

(1) *Femtochemistry*; Zewail, A. H., Ed.; World Scientific: Singapore, 1994; Vol. I, II.
(2) *Femtosecond Chemistry*; Manz, J., Wöste, L., Eds.; VCH: Heidelberg, 1995.
(3) *Femtochemistry: Ultrafast Chemical and Physical Processes in Molecular Systems*; Chergui, M., Ed.; World Scientific: Singapore, 1996.
(4) Manz, J. Molecular Wave packet Dynamics: Theory for Experiments 1926−1996. In *Femtochemistry and Femtobiology*; Sundström, V., Ed.; World Scientific: Singapore, 1997; pp 98−99 (in press).
(5) Dyne, P. J.; Style, D. W. G. *J. Chem. Soc.* **1952**, 2122.
(6) Style, D. W. G.; Ward, J. C. *J. Chem. Soc.* **1952**, 2125.
(7) Black, G. "Research on High Energy Storage for Laser Amplifiers", Stanford Research Institute, 1976.
(8) Okabe, H.; Kawasaki, M.; Tanaka, Y. *J. Chem. Phys.* **1980**, *73*, 6162.
(9) Fotakis, C.; Martin, M.; Donovan, R. J. *J. Chem. Soc., Faraday Trans.* **1982**, *78*, 1363.
(10) Okabe, H. *Photochemistry of Small Molecules*; Wiley: New York, 1978.
(11) Okabe, H.; Laufer, A. H.; Ball, J. J. *J. Chem. Phys.* **1971**, *55*, 373.
(12) Butler, L. J.; Hintsa, E. J.; Shane, S. F.; Lee, Y. T. *J. Chem. Phys.* **1987**, *86*, 2051.
(13) Baumert, T.; Herek, J. L.; Zewail, A. H. *J. Chem. Phys.* **1993**, *99*, 4430.
(14) Ludowise, P.; Blackwell, M.; Chen, Y. *Chem. Phys. Lett.* **1997**, *273*, 211−218.
(15) Marvet, U.; Dantus, M. *Chem. Phys. Lett.* **1996**, *256*, 57.
(16) Marvet, U.; Dantus, M. Femtosecond Dynamics of Concerted Elimination Processes. In *Femtochemistry: Ultrafast Chemical and Physical Processes in Molecular Systems*; Chergui, M., Ed.; World Scientific: Singapore, 1996; pp 134−137.
(17) Zhang, Q.; Marvet, U.; Dantus, M. Concerted Elimination Dynamics from Highly Excited States. *Faraday Discuss.* **1997**, *108*, xxxx.
(18) Mrozowski, S. *Z. Phys.* **1937**, *106*, 458.
(19) Doyle, R. O. *J. Quant. Spectrosc. Radiat. Transfer* **1968**, *8*, 1555.
(20) Dubov, V. S.; Gudzenko, L. I.; Gurvich, L. V.; Iokovlenko. *Chem. Phys. Lett.* **1977**, *45*, 330.
(21) Lidov, D. B.; Fakone, R. W.; Young, T. F.; Harris, S. E. *Phys. Rev.* **1976**, *36*, 462.

(22) Inoue, G.; Ku, J. K.; Setser, D. W. *J. Chem. Phys.* **1984**, *80*, 6006.
(23) Schloss, J. H.; Jones, R. B.; Eden, J. G. *J. Chem. Phys.* **1993**, *99*, 6483.
(24) Jones, R. B.; Schloss, J. H.; Eden, J. G. *J. Chem. Phys.* **1993**, *98*, 4317.
(25) Gordon, E. B.; Egorov, V. G.; Nalivaiko, S. E.; Pavlenko, V. S.; Rzhevsky, O. S. *Chem. Phys. Lett.* **1995**, *242*, 75.
(26) Bergeman, T.; Liao, P. *J. Chem. Phys.* **1980**, *72*, 886.
(27) Scheingraber, H.; Vidal, C. R. *J. Chem. Phys.* **1977**, *66*, 3694.
(28) Miller, J. D.; Cline, R. A.; Heinzen, D. J. *Phys. Rev. Lett.* **1993**, *71*, 2204.
(29) Napolitano, R.; Weiner, J.; Williams, C. J.; Julienne, P. S. *Phys. Rev. Lett.* **1994**, *73*, 1352.
(30) Lett, P. D.; Julienne, P. S.; Philips, W. D. *Annu. Rev. Phys. Chem.* **1995**, *46*, 423.
(31) Thorsheim, H. R.; Weiner, J.; Julienne, P. S. *Phys. Rev. Lett.* **1987**, *58*, 2420.
(32) Cline, R. A.; Miller, J. D.; Heinzen, D. J. *Phys. Rev. Lett.* **1994**, *73*, 632.
(33) Machholm, M.; Giusti-Suzor, A.; Mies, F. H. *Phys. Rev. A* **1994**, *50*, 5025.
(34) Petsalakis, I. D.; Mercouris, T.; Nicolaides, C. A. *Chem. Phys.* **1994**, *189*, 615.
(35) Mercouris, T.; Petsalakis, I. D.; Nicolaides, C. A. *Chem. Phys. Lett.* **1993**, *208*, 197.
(36) Potter, E. D.; Herek, J. L.; Pedersen, S.; Lin, Q.; Zewail, A. H. *Nature* **1992**, *355*, 66.
(37) Scherer, N. F.; Khundkar, L. R.; Bernstein, R. B.; Zewail, A. H. *J. Chem. Phys.* **1987**, *87*, 1451.
(38) Sims, R.; Gruebele, M.; Potter, E. D.; Zewail, A. H. *J. Chem. Phys.* **1992**, *97*, 4127.
(39) Ionov, S. I.; Brucker, G. A.; Jaques, C.; Valachovic; Wittig, C. *J. Chem. Phys.* **1993**, *99*, 6553.
(40) Zhong, D.; Cheng, P. Y.; Zewail, A. H. *J. Chem. Phys.* **1996**, *105*, 7864.
(41) Visticot, J. P.; Soep, B.; Whitham, C. J. *J. Phys. Chem.* **1988**, *92*, 4574.
(42) Marvet, U.; Dantus, M. *Chem. Phys. Lett.* **1995**, *245*, 393.
(43) Marvet, U.; Dantus, M. Femtosecond photoassociation spectroscopy: coherent bond formation. In *Femtochemistry: Ultrafast Chemical and Physical Processes in Molecular Systems*; Chergui, M., Ed.; World Scientific: Singapore, 1996; pp 138−142.
(44) Backhaus, P.; Manz, J.; Schmidt, B. *Adv. Chem. Phys.* **1997**.
(45) Backhaus, P.; Schmidt, B. *Chem. Phys.* **1997**, *217*, 131−143.
(46) Gross, P.; Dantus, M. *J. Chem. Phys.* **1997**, *106*, 8013.
(47) Korolkov, M. V.; Manz, J.; Paramonov, G. K.; Schmidt, B. *Chem. Phys. Lett.* **1996**, *260*, 604.
(48) Values obtained from: Lide, D. R.; et al. *Handbook of Chemistry and Physics*, 74th ed.; CRC: Boca Raton, FL, 1993.
(49) Tellinghuisen, J. *J. Mol. Spectrosc.* **1982**, *94*, 231.
(50) Zheng, X.; Fei, S.; Heaven, M. C.; Tellinghuisen, J. *J. Chem. Phys.* **1992**, *96*, 4877.
(51) Heemann, U.; Knockel, H.; Tiemann, E. *Chem. Phys. Lett.* **1982**, *90*, 17.
(52) Wilson, P. J.; Ridley, T.; Lawley, K. P.; Donovan, R. J. *Chem. Phys.* **1994**, *182*, 325.
(53) Kawasaki, M.; Lee, S. J.; Bersohn, R. *J. Chem. Phys.* **1975**, *63*, 809.
(54) Baughcum, S. L.; Leone, S. R. *J. Chem. Phys.* **1980**, *72*, 6531.
(55) Baskin, J. S.; Zewail, A. H. *J. Phys. Chem.* **1994**, *98*, 3337.
(56) Cain, S. R.; Hoffmann, R.; Grant, E. R. *J. Phys. Chem.* **1981**, *85*, 4046.
(57) Zhenacker, A.; Duval, M. C.; Jouvet, C.; Ladeux-Dedonder, C.; Solgadi, D.; Soep, B.; Bonoist d'Azy, O. *J. Chem. Phys.* **1987**, *86*, 6565.
(58) Koperski, J.; Atkinson, J. B.; Krause, L. *Can. J. Phys.* **1994**, *72*, 1070.
(59) Stock, M.; Smith, E. W.; Drullinger, R. E.; Hessel, M. M. *J. Chem. Phys.* **1978**, *68*, 4167.
(60) Drullinger, R. E.; Hessel, M. M.; Smith, E. W. *J. Chem. Phys.* **1977**, *66*, 5656.
(61) The Franck−Condon factors are calculated by evaluating the square of the overlap integrals between the *bound* vibrational levels in the ground electronic state and the levels in the D 1_u state.
(62) Gordon, R. G. *J. Chem. Phys.* **1966**, *45*, 1643.
(63) Levine, R. D.; Bernstein, R. B. *Molecular Reaction Dynamics and Chemical Reactivity*; Oxford University Press: New York, 1987.